2010 American Control Conference
Marriott Waterfront, Baltimore, MD, USA
June 30-July 02, 2010

Fault-Tolerant Control of Sampled-Data Nonlinear Distributed Parameter Systems

Sathyendra Ghantasala and Nael H. El-Farra†
Department of Chemical Engineering & Materials Science
University of California, Davis, CA 95616 USA

Abstract— **This work presents an integrated fault detection and fault-tolerant control architecture for spatially-distributed systems described by highly-dissipative systems of nonlinear partial differential equations with actuator faults and sampled measurements. The architecture consists of a family of nonlinear feedback controllers, observer-based fault detection filters that account for the discrete measurement sampling, and a switching law that reconfigures the control actuators following fault detection. An approximate model that captures the dominant dynamics of the infinite-dimensional system is embedded in the control system to provide the controller and fault detection filter with estimates of the measured output between sampling instances. The model state is then updated using the actual measurements whenever they become available from the sensors. A sufficient condition for stability of the sampled-data nonlinear closed-loop system is derived in terms of the sampling rate, the model accuracy, the controller design parameters and the spatial placement of the control actuators. This characterization is used to derive rules for fault detection and actuator reconfiguration. The results are demonstrated through an application to the problem of stabilizing the zero solution of the Kuramoto-Sivashinsky equation.**

I. Introduction

Compared with the extensive body of literature on fault diagnosis and fault-tolerant control for lumped parameter systems described by ordinary differential equations (e.g., see [1], [2], [3]), results for spatially-distributed systems have been limited (e.g., see [4], [5], [6]). Major bottlenecks in the design of fault-tolerant control systems for distributed parameter systems include the infinite-dimensional nature of these systems, as well as their complex dynamics characterized by nonlinearities and uncertainties. Recently, we developed in [7], [8], [9], [10] a framework for the integration of model-based fault detection, isolation and control system reconfiguration for distributed processes modeled by nonlinear parabolic PDEs with control constraints and actuator faults. The framework brings together tools from infinite-dimensional systems, model reduction, nonlinear and robust control, as well as hybrid system theory.

Beyond the problems of uncertainty and constraints, one of the key issues that needs to be accounted for in the design of monitoring and fault-tolerant control systems is the issue of measurement sampling. In practice, measurements of the process outputs are typically available from the sensors at discrete times and not continuously. The limitations on the frequency of measurement availability imposes restrictions on the implementation of the feedback controller and can also erode the diagnostic and fault-tolerance capabilities of the control system if not explicitly accounted for at the design stage. An effort to address this problem was initiated in [11] where a fault detection and fault-tolerant control architecture for distributed processes modeled by linear systems of parabolic PDEs with a limited number of measurements that are sampled at discrete times was developed. A key idea – inspired by the results in [12] and [13] on model-based control of networked systems – is to embed within the fault-tolerant control system an approximate model of the dominant process modes to provide the observer with estimates of the outputs between sampling instances. By exploiting the linear structure of the process and the controllers, both necessary and sufficient conditions for closed-loop stability were obtained. Since many transport-reaction processes and fluid dynamic systems are characterized by strong nonlinear dynamics and need to be operated over wide regions of the operating space, it is important to develop sampled-data fault-tolerant control systems that account explicitly for the nonlinearities – both in the design of control laws and the development of fault diagnosis and reconfiguration schemes.

Motivated by these considerations, we develop in this work an integrated fault detection and fault-tolerant control architecture for spatially-distributed systems described by highly-dissipative nonlinear PDEs with sampled measurements and actuator faults. The rest of the paper is organized as follows. Following some preliminaries, an approximate finite-dimensional model that captures the dominant dynamics is obtained and used in Section III to design a stabilizing feedback controller. The sampled-data closed-loop system is then formulated as a discrete jump system, and an explicit characterization of the minimum allowable sampling rate that guarantees closed-loop stability in the absence of faults is obtained. This characterization is then used in Section IV to derive fault detection and actuator reconfiguration laws for a given sampling rate. Finally, the proposed methodology is applied in Section V to the problem of actuator fault-tolerant stabilization of the spatially-uniform unstable steady-state of the Kuramoto-Sivashinsky equation.

II. Preliminaries

A. Mathematical description

As an example of highly-dissipative nonlinear PDEs that will be used to demonstrate the design and implementation

† To whom correspondence should be addressed: E-mail: nhelfarra@ucdavis.edu. Financial support by ACS-PRF grant, 47072-G9, is gratefully acknowledged.

of the proposed fault detection and reconfiguration methodology, we consider the one-dimensional KSE equation with distributed control and actuator faults:

$$\frac{\partial U}{\partial t} = -\nu\frac{\partial^4 U}{\partial z^4} - \frac{\partial^2 U}{\partial z^2} - cU\frac{\partial U}{\partial z} + \sum_{i=1}^{l} b_i^k(z)[u_i^k(t) + f_{a,i}^k(t)], \quad k \in \mathcal{C} = \{1, 2, \cdots, N\} \tag{1}$$

$$y_\kappa(t) = \int_{-\pi}^{\pi} q_\kappa(z)U(z,t)dz, \ \kappa = 1, \ldots, m \tag{2}$$

subject to the boundary and initial conditions:

$$\frac{\partial^j U}{\partial z^j}(-\pi, t) = \frac{\partial^j U}{\partial z^j}(\pi, t), j = 0, \ldots, 3, U(z, 0) = U_0(z) \tag{3}$$

where $U(z,t)$ is the state of the system, $z \in [-\pi, \pi]$ is the spatial coordinate, t is the time, $\nu > 0$ is the instability parameter, $c > 0$ is a positive real constant, $u_i^k(t) \in \mathbb{R}$ is the i-th manipulated input associated with the k-th control configuration, $f_{a,i}^k(t)$ is a fault in the i-th actuator of the k-th control configuration, l is the total number of manipulated inputs, $b_i^k(z)$ is the i-th actuator distribution function which determines how the control action computed by the i-th control actuator is distributed (e.g., point or distributed actuation) in the spatial interval $[-\pi, \pi]$), k is a discrete index that takes values in a finite set $\mathcal{C}$ and represents the active control configuration, $y_\kappa \in \mathbb{R}$ denotes the κ-th measured output, and $q_\kappa(z)$ is the sensor distribution function which determines the location and type of the measurement sensors (e.g., point or distributed sensing).

Remark 1: The KSE represents a simple model that describes incipient instabilities in a variety of physical and chemical systems, including falling liquid films, unstable flame fronts, Belouzov-Zabotinskii reaction patterns and interfacial instabilities between two viscous fluids. Compared with the significant research work on the dynamics and control of the KSE with periodic boundary conditions (e.g., [14], [15], [16], [17]), results on fault diagnosis and handling in the KSE are limited at present [5].

B. Formulation of the infinite-dimensional system

Using standard techniques from operator theory, the PDE of Eqs.1-3 can be formulated as an infinite-dimensional-system of the following form:

$$\begin{aligned} \dot{x} &= \mathcal{A}x + \mathcal{B}^k[u^k(t) + f_a^k(t)] + f(x), \quad x(0) = x_0 \\ y &= \mathcal{Q}x \end{aligned} \tag{4}$$

where $\mathcal{A}$ is the differential operator, $\mathcal{B}^k$ is the input operator, $f(x)$ is a smooth nonlinear function and $\mathcal{Q}$ is the measurement operator.For $\mathcal{A}$, the eigenvalue problem can be formulated as:

$$\mathcal{A}\phi_n = -\nu\frac{\partial^4 \phi_n}{\partial z^4} - \frac{\partial^2 \phi_n}{\partial z^2} = \lambda_n \phi_n, \quad n = 1, \ldots, \infty \tag{5}$$

subject to:

$$\frac{\partial^j \phi_n}{\partial z^j}(-\pi) = \frac{\partial^j \phi_n}{\partial z^j}(+\pi), \quad j = 0, \ldots, 3 \tag{6}$$

where λ_n denotes an eigenvalue and ϕ_n denotes an eigenfunction. It can be shown by a direct computation of the solution of the above eigenvalue problem that, for a fixed value of ν, $\mathcal{A}$ has a real pure point spectrum, the number of unstable eigenvalues of $\mathcal{A}$ is finite and the distance between two consecutive eigenvalues (i.e., λ_n and λ_{n+1}) increases as n increases. Furthermore, for a fixed value of $\nu > 0$, the spectrum can be partitioned as $\sigma(\mathcal{A}) = \sigma_1(\mathcal{A}) \bigcup \sigma_2(\mathcal{A})$, where $\sigma_1(\mathcal{A})$ contains the first m (for some finite m) "slow" eigenvalues (i.e., $\sigma_1(\mathcal{A}) = \{\lambda_1, \ldots, \lambda_m\}$) and $\sigma_2(\mathcal{A})$ contains the remaining "fast" eigenvalues (i.e., $\sigma_2(\mathcal{A}) = \{\lambda_{m+1}, \ldots\}$ where $\lambda_{m+1} < 0$), and the separation between the "slow" and "fast" eigenvalues is characterized by the parameter $\epsilon = |\lambda_1|/|\lambda_{m+1}|$. The separation between the "slow" and "fast" eigenvalues suggests that the dominant dynamics of the KSE can be described by a finite-dimensional system and motivates applying model reduction techniques to the system of Eq.4 to derive an approximate finite-dimensional system.

C. Modal decomposition

Let $\mathcal{H}_s$, $\mathcal{H}_f$ be modal subspaces of $\mathcal{A}$, defined as $\mathcal{H}_s = \text{span}\{\phi_1, \ldots, \phi_m\}$ and $\mathcal{H}_f = \text{span}\{\phi_{m+1}, \phi_{m+2}, \ldots\}$. Defining the orthogonal projection operators, $\mathcal{P}_s$ and $\mathcal{P}_f$, such that $x_s = \mathcal{P}_s x$, $x_f = \mathcal{P}_f x$, the state of the system of Eq.4 can be decomposed as $x = x_s + x_f$. Applying $\mathcal{P}_s$ and $\mathcal{P}_f$ to the system of Eq.4 and using the decomposition of x, the system of Eq.4 can be decomposed as:

$$\dot{x}_s = \mathcal{A}_s x_s + \mathcal{B}_s^k[u^k + f_a^k] + f_s(x_s, x_f), x_s(0) = \mathcal{P}_s x_0 \tag{7}$$

$$\dot{x}_f = \mathcal{A}_f x_f + \mathcal{B}_f^k[u^k + f_a^k] + f_f(x_s, x_f), x_f(0) = \mathcal{P}_f x_0 \tag{8}$$

$$y = \mathcal{Q}x_s + \mathcal{Q}x_f \tag{9}$$

where $\mathcal{A}_s = \mathcal{P}_s\mathcal{A}$ is an $m \times m$ diagonal matrix of the form $\mathcal{A}_s = \text{diag}\{\lambda_j\}$, $\mathcal{B}_s^k = \mathcal{P}_s\mathcal{B}^k$, $\mathcal{A}_f = \mathcal{P}_f\mathcal{A}$ is an unbounded differential operator which is exponentially stable (following from the fact that $\lambda_{m+1} < 0$ and the selection of $\mathcal{H}_s$ and $\mathcal{H}_f$), $\mathcal{B}_f^k = \mathcal{P}_f\mathcal{B}^k$. Neglecting the fast and stable x_f-subsystem of Eq.8, the following approximate, m-dimensional slow system is obtained:

$$\dot{\bar{x}}_s = \mathcal{A}_s\bar{x}_s + \mathcal{B}_s^k[u^k + f_a^k] + f_s(\bar{x}_s, 0), \quad \bar{y} = \mathcal{Q}\bar{x}_s \tag{10}$$

where the bar symbols denote that these variables are associated with a finite-dimensional system. To facilitate the controller synthesis and simplify closed-loop analysis, we will consider in the remainder of the paper that the inverse (or pseudo-inverse in the case of a non-square system) of the operator $\mathcal{Q}$ exists. This requirement, which can be met by appropriate choice of the locations of the measurement sensors, allows obtaining estimates of the state of the finite-dimensional system of Eq.10 from the measurements.

III. Design and analysis of finite-dimensional sampled-data control system

A. Model-based controller synthesis

To realize the desired sampled-data control structure, we will first synthesize in this part a nonlinear controller that stabilizes the finite-dimensional system in the absence of sampling constraints (i.e., when the sensors transmit their data continuously to the controller). To facilitate controller synthesis, we consider the following representation of the

approximate finite-dimensional system which describes explicitly the evolution of the amplitudes of the dominant (slow) eigenmodes:

$$\dot{a}_s = Fa_s + \bar{G}^k(z_a)[u^k + f_a^k] + h(a_s),\ \bar{y} = Q_s(z_s)a_s \quad (11)$$

where $a_s(t) = [a_1(t) \cdots a_m(t)]' \in \mathbb{R}^m$, $a_i(t)$ is the amplitude of the i-th eigenmode, $\bar{x}_s(t) = \sum_{j=1}^m a_j(t)\phi_j(z)$, $(\bar{x}_s(t), \phi_j) = a_j(t)(\phi_j, \phi_j)$, F is an $m \times m$ diagonal matrix of the form $F = \text{diag}\{\lambda_j\}$, $\bar{G}^k(z_a)$ is an $m \times l$ matrix whose (i,j)-th element is given by $G_{ij}^k = (b_j^k(z), \phi_i(z))$ which is parameterized by the location of the control actuators, $h(\cdot) = [h_1(\cdot)\ h_2(\cdot)\ \cdots\ h_m(\cdot)]'$, $h_j = (f_s(\bar{x}_s, 0), \phi_j)$ is a smooth nonlinear function of its argument, and Q_s is an $m \times m$ invertible matrix whose (i,j)-th element is given by $Q_{ij} = (q_i(z), \phi_j(z))$ and is parameterized by the locations of the measurement sensors. Note from the definition of a_s that stabilization of the system of Eq.11 implies stabilization of the system of Eq.10.

To proceed with controller synthesis, we will consider that an uncertain finite-dimensional model of the fault-free system of Eq.11 is available:

$$\dot{w} = \widehat{F}w + \widehat{G}^k(z_a)u^k + \widehat{h}(w),\ \ \widehat{y}(t) = Q_s(z_s)w(t) \quad (12)$$

where w is the state of a model that generates an estimate of a_s, and $\widehat{F}$, $\widehat{G}^k(\cdot)$, $\widehat{h}(\cdot)$ are models of F, $G^k(\cdot)$ and $h(\cdot)$, respectively. Notice that in general $\widehat{F} \neq F$, $\widehat{G}^k \neq G^k$ and $\widehat{h} \neq h$ to allow for possible plant-model mismatch.

Assumption 1: *For each $k \in \mathcal{C}$, there exists a nonlinear feedback control law of the general form:*

$$u^k = p^k(w) \quad (13)$$

such that the origin of the closed-loop model of Eqs.12-13 satisfies:

$$\| w(t) \| \leq \alpha^k \| w(t_0) \| e^{-\beta^k(t-t_0)} \quad (14)$$

for some $\alpha^k \geq 1$, $\beta^k > 0$, for all $w(t_0) \in \Omega^k$, for some compact neighborhood $\Omega^k \subset \mathbb{R}^m$ containing the origin in its interior.

B. Controller implementation under sampling

To deal with the unavailability of continuous measurements, the dynamic model of Eq.12 is embedded in the control system to provide the controller with an estimate of the state measurements in between sampling times. The state of the model is then updated using the actual measurements whenever they become available from the sensors. The model-based controller is implemented as follows:

$$\begin{aligned} u^k(t) &= p^k(w(t)),\ \ t \in (t_j, t_{j+1}) \\ \dot{w}(t) &= \widehat{F}w(t) + \widehat{G}^k(z_a)u^k(t) + \widehat{h}(w(t)) \\ \widehat{y}(t_j) &= \bar{y}(t_j),\ j = 0, 1, 2, \cdots \end{aligned} \quad (15)$$

where $\widehat{y}$ is an estimate of $\bar{y}$, w is an estimate of a_s, and $\Delta := t_{j+1} - t_j$ is the sampling period. Note that since Q_s is invertible (or pseudo-invertible in the case of a non-square system), re-setting the output of the model to match the output of the finite-dimensional slow system is equivalent to re-setting the state of the model since $w(t_j) = Q_s^{-1}\bar{y}(t_j)$.

C. Closed-loop stability analysis

To characterize the maximum allowable sampling period (equivalently, the minimum sampling rate) between the sensors and the controller, we define the model estimation error as $e_s(t) = a_s(t) - w(t)$, where $e_s \in \mathbb{R}^m$. The overall fault-free closed-loop system can then be formulated as a combined discrete-continuous system and written in the following form:

$$\begin{aligned} \dot{a}_s(t) &= Fa_s(t) + G^k(z_a)p^k(w(t)) + h(a_s(t)) \\ \dot{w}(t) &= \widehat{F}w(t) + \widehat{G}^k(z_a)p^k(w(t)) + h(w(t)) + \Theta(w(t)) \\ \widehat{y}_s(t) &= Q_s w(t),\ t \in (t_j + t_{j+1}) \\ e_s(t_j) &= 0,\ j = 0, 1, 2, \cdots,\ \Delta = t_{j+1} - t_j \end{aligned} \quad (16)$$

where $\Theta(w) = \widehat{h}(w) - h(w)$. Note that while the state of the slow subsystem, a_s evolves continuously in time, the error e_s is reset to zero at each transmission instance since the state of the model is updated every Δ seconds using the output measurement. Referring to Eq.16, it is clear that the right hand-side depends on the slow system dynamics, the model and the control law. Since the functions $\widehat{h}(\cdot)$, $h(\cdot)$ and $p^k(\cdot)$ are assumed to be sufficiently smooth, it follows that there exist positive real constants L_h, L_δ and L_p such that the following estimates hold for all $x, y \in \Omega$ (see Assumption 1):

$$\begin{aligned} \| h(x) - h(y) \| &\leq L_h \| x - y \| \\ \| \Theta(x) - \Theta(y) \| &\leq L_\Theta \| x - y \| \\ \| p^k(x) - p^k(y) \| &\leq L_p^k \| x - y \| \end{aligned} \quad (17)$$

Note that if the model is accurate, L_Θ will be small. The following theorem provides a sufficient condition for the stability of the sampled-data finite-dimensional closed-loop system in terms of the sampling period, the model uncertainty, the controller design parameters and the control actuator locations. The proof can be sketched along the lines of the proof of the Theorem 1 in [18] and is omitted for brevity.

Theorem 1: *Consider the closed-loop system of Eq.11 with $f_a^k \equiv 0$ subject to the control and update laws of Eq.15, and the compensated model of Eq.12 for which Assumption 1 holds, with $a_s(t_0) = w(t_0) \in \Omega$. Then, if*

$$F_1^k(\Delta) := 1 - \alpha^k \left(e^{-\beta^k \Delta} + (e^{L_e \Delta} - e^{-\beta^k \Delta}) \frac{L_w^k}{\beta^k + L_e} \right) > 0 \quad (18)$$

the states of the sampled-data closed-loop system are bounded and satisfy:

$$\| a_s(t_{j+1}^-) \| < \| a_s(t_j) \| \ \text{ for all } \ \| a_s(t_j) \| > r^k(\Delta) \quad (19)$$

for $j = 0, 1, 2, \cdots$, where $r^k(\Delta) = F_2^k(\Delta)/F_1^k(\Delta)$,

$$F_2^k(\Delta) = \frac{L_0^k}{L_e}(e^{L_e \Delta} - 1) \quad (20)$$

and $L_e = (L_h + \| \widehat{F} \| + \| \widetilde{F} \|)$, $\widetilde{F} = F - \widehat{F}$, $L_w^k = L_\Theta + \| \widetilde{F} \| + \| \widetilde{G}^k \| L_p^k$, $\widetilde{G}^k = G^k - \widehat{G}^k$, and $L_0^k = (\| \widetilde{G}^k \| \| p^k(0) \| + \| \Theta(0) \|)$. Furthermore, $\lim_{t \to \infty} \|a_s(t)\| \leq \gamma_1^k r^k(\Delta) + \gamma_2^k$, where $\gamma_1^k = \max_{t - t_j \in [0,h]} 1 - F_1^k(t - t_j)$ and $\gamma_2^k = \max_{t - t_j \in [0,h]} F_2^k(t - t_j)$.

Remark 2: Theorem 1 establishes that if the sampling period is chosen such that Eq.18 is satisfied, the norm of the state of the closed-loop finite-dimensional slow system is guaranteed to decrease at successive sampling times as long as the sampled state is outside some terminal neighborhood of the origin $r^k(\Delta)$ (the size of which is fixed by the choice of the sampling period). This implies that the sampled closed-loop state is guaranteed to converge in finite time to the terminal set where it remains confined for all future times. Note that between consecutive updates the state is always bounded and can grow only a certain amount (since $t - t_j < \Delta$) and this growth is independent of j.

Remark 3: In the particular case when the origin is an equilibrium point of both the slow system and the model (i.e., the model uncertainty is vanishing), it can be shown that the closed-loop state is not only bounded but is also guaranteed to converge to the origin as time tends to infinity, i.e., the sampled-data closed-loop system is asymptotically stable at the origin. Specifically, when the model uncertainty is vanishing, we have $\Theta(0) = 0$ and $p^k(0) = 0$ which implies that $L_0^k = 0$ and, consequently, $F_2^k(\Delta) = 0$ and $r^k(\Delta) = 0$. The terminal set thus collapses to the origin in this case and $\lim_{t\to\infty} \|a_s(t)\| = 0$ (see Section V for an example).

Remark 4: It can be seen from the expressions in Eq.18 and Eq.20 that the given bound on the minimum stabilizing sampling rate is dependent on the degree of mismatch between the dynamics of the approximate system and the model used to describe it. Given bounds on the size of the uncertainty, the stability criterion of Theorem 1 can be used to estimate the range of stabilizing sampling periods. Alternatively, if Δ is fixed by the characteristics of the sensing device, it is possible to use the stability condition to obtain a bound on the maximum tolerable process-model mismatch. In addition to model uncertainty, the stabilizing sampling period depends on the controller design parameters (whose effect is reflected in α^k and β^k) as well as on the locations of the control actuators (due to the parametrization of G^k by the actuator location).

IV. Fault-tolerant control system design

A. Observer-based fault detection

The main idea here is to design a state observer for the fault-free finite-dimensional system and use it as a fault detection filter by comparing its output with the actual output of the system to determine the fault or health status of the control actuators. To this end, and based on the finite-dimensional model of Eq.12, we consider a fault detection filter of the form:

$$\dot{\eta}(t) = \widehat{F}\eta(t) + \widehat{G}_s^k u^k(t) + \widehat{h}(\eta(t)) + L(\widehat{y}(t) - Q_s\eta(t)) \qquad (21)$$

where $\widehat{y}(t) = Q_s w(t)$, $\widehat{y}(t_j) = \bar{y}(t_j)$, for $j = 0, 1, 2, \cdots$, and L is an observer gain chosen such that $\widehat{F} - LQ_s$ is Hurwitz. The residual, which captures the discrepancy between the output of the slow system and the output of the observer, is defined as:

$$r_s(t) = \|\bar{y}(t) - Q\eta(t)\| \qquad (22)$$

To generate an estimate of the state, the above fault detection filter uses the output of the model of Eq.12 when measurements of the actual output are not available. The model output (and state) is then re-set based on the measurements when they become available. The following proposition characterizes the expected fault-free evolution of the residual which is then used for fault detection.

Proposition 1: *Consider the closed-loop system of Eq.11 and Eq.15 with $f_a^k \equiv 0$ for a fixed $k \in \mathcal{C}$, where the sampling period Δ is chosen such that Eq.18 holds. Consider also the fault detection filter of Eq.21 for a fixed $k \in \mathcal{C}$. Then, there exist a class $\mathcal{KL}$ function, $\beta_0(\cdot,\cdot)$, a class $\mathcal{K}$ function, $\gamma_0(\cdot)$, and a positive constant k_1 such that the residual defined by Eq.22 satisfies a time-varying bound of the form:*

$$\|r_s(t)\| \leq \beta_0(\|r_s(t_0)\|, t - t_0) + \gamma_0\Big(\sup_{t_0\leq\tau\leq t} \|\Gamma^k(\xi^k(\tau))\|\Big) \qquad (23)$$

for all $t \geq t_0$ and for all $\|r_s\| \leq k_1$, where $\xi = [a_s\ w]'$ and $\Gamma^k(\xi) = (\widetilde{F} + LQ_s)a_s - \Theta(a_s) + \widetilde{G}^k p^k(w) - LQ_s w$.

Proof: From the definition of the residual, we have $\dot{r}_s = \dot{a}_s - \dot{\eta}$. Substituting for $\dot{a}_s$ and $\dot{\eta}$ from Eq.11 and Eq.21, respectively, and using the definitions of ξ and $\Gamma(\xi)$ given in the statement of the theorem yields:

$$\dot{r}_s = \widehat{F}_o r_s + \widehat{h}(a_s) - \widehat{h}(\eta) + \Gamma^k(\xi) \qquad (24)$$

From the fact that $\widehat{F}_o := \widehat{F} - LQ_s$ is Hurwitz, it follows that for any positive-definite symmetric matrix M, there exists a positive-definite symmetric solution $P > 0$ that satisfies the matrix Lyapunov equation $\widehat{F}_o^T P + P\widehat{F}_o = -M$. Using $V = r_s^T P r_s$ as a Lyapunov function candidate, the time-derivative of $V(r_s)$ along the trajectories of the system of Eq.24 can be computed as follows:

$$\dot{V}(r_s) = -r_s^T M r_s + 2r_s^T P(\widehat{h}(a_s) - \widehat{h}(\eta)) + 2r_s^T P\Gamma^k(\xi) \qquad (25)$$

From the properties of the function $\widehat{h}(\cdot)$, it follows that there exists a positive constant k_1 such that $\|\widehat{h}(a_s) - \widehat{h}(\eta)\| \leq \widehat{L}_h\|r_s\|$ for all $\|r_s\| \leq k_1$. Substituting this estimate into Eq.25, it can be shown after some manipulations that:

$$\begin{aligned} \dot{V}(r_s) &\leq -c_1\|r_s\|^2 + c_2\|r_s\|\|\Gamma^k(\xi)\| \\ &\leq -\tfrac{c_1}{2}\|r_s\|^2 \quad \forall\ \|r_s\| \geq 2c_1^{-1}c_2\|\Gamma^k(\xi)\| \end{aligned} \qquad (26)$$

where $c_1 = \lambda_{\min}(M) + 2\lambda_{\max}(P)\widehat{L}_h > 0$, $c_2 = 2\lambda_{\max}(P) > 0$, $\lambda_{\min}(M)$ is the minimum eigenvalue of M and $\lambda_{\max}(P)$ is the maximum eigenvalue of P. Therefore, the system of Eq.24 is input-to-state stable with respect to $\Gamma^k(\xi)$. Recall from Theorem 1 that when Eq.18 is satisfied, both w and a_s are bounded and therefore $\Gamma^k(\xi)$ is also bounded. From the definition of input-to-state stability [19], we finally conclude that there exist a class $\mathcal{KL}$ function β_0, a class $\mathcal{K}$ function γ_0 such that Eq.23 is satisfied. This completes the proof of the proposition.

Remark 5: Based on the result of Proposition 1, and for a given sampling rate (chosen to be stabilizing in the absence of faults), a fault can be declared if the residual breaches the time-varying threshold of Eq.23 at some time. Note, however, that even though η is available continuously, the fact that $\bar{y}$ is available only at the sampling times implies

that the residual can be evaluated only at those times and not continuously, i.e., fault detection can take place only at $t_j,\ j = 0, 1, 2, \cdots$ regardless of when the fault actually occurs. Detection delays can be minimized by tightening the bound on r_s which can be achieved by proper selection of the controller and observer design parameters.

B. Actuator reconfiguration logic

Once a fault is detected in the operating actuator configuration, the supervisor needs to determine which fall-back configuration to select and activate in order to preserve closed-loop stability. The following theorem describes the actuator reconfiguration logic. The proof follows directly from the result of Theorem 1 and is omitted for brevity.

Theorem 2: *Consider the closed-loop system of Eq.11 and Eq.15, with $k(t_0) = i$ for some $i \in \mathcal{K}$ and a sampling period Δ chosen such that Eq.18 is satisfied. Let T_f be the earliest time that $f_a^i(T_f) \neq 0$. Then the switching rule:*

$$k(t) = \left\{ \begin{array}{ll} i, & 0 \leq t < T_f \\ \nu \neq i, & t \geq T_f,\ F_1^\nu(\Delta) > 0 \end{array} \right\} \qquad (27)$$

guarantees that the states of the closed-loop system remain bounded and $\lim_{t\to\infty} \|a_s(t)\| \leq \gamma_1^\nu r(\Delta) + \gamma_2^\nu$.

Remark 6: While the sampled-data fault-tolerant control system developed in Sections III-IV is designed on the basis of the finite-dimensional system of Eq.11, it can be shown that this architecture continues to enforce stability and fault-tolerance when implemented on the infinite-dimensional system of Eqs.7-9 provided that the separation between the slow and fast states is sufficiently large (i.e., for ϵ small enough), and the fault detection threshold is appropriately modified to account for the approximation errors resulting from neglecting x_f in the finite-dimensional system. This argument can be justified using techniques from singular perturbations for infinite-dimensional systems [20].

V. Simulation study: Application to the Kuramoto-Sivashinsky equation

In this section, we demonstrate the application of the fault detection and fault-tolerant control methodology described in the previous sections to the problem of stabilizing the zero solution of the one-dimensional KSE with periodic boundary conditions described by Eqs.1-3. For simplicity, we consider the KSE in the space of odd functions with spatial zero mean. The eigenvalue problem for the differential operator in this space yields $\lambda_j = -\nu j^4 + j^2$, $\phi_j(z) = \sqrt{\frac{1}{\pi}}\sin(jz)$, $j = 1, \ldots, \infty$. It can be verified that for $\nu = 0.2$ the first two eigenvalues are unstable and the spatially-uniform zero steady-state is unstable. The control objective is to stabilize the system at this unstable steady state using two point control actuators (with finite support) and two point measurement sensors. We consider the first two eigenvalues to be the dominant ones and use standard Galerkin's method to derive the a second-order system of the form of Eq.11 that describes the temporal evolution of the amplitudes of the first two eigenmodes, where $U(z,t) = \sum_{i=1}^{\infty} a_i(t)\phi_i(z)$, $F = \mathrm{diag}\{\lambda_1, \lambda_2\}$, $\lambda_1 = \lambda_2 = 0.8$ and

$$G^k = \frac{1}{2\mu}\left[\begin{array}{ll} \phi_1'(z_1-\mu) - \phi_1'(z_1+\mu) & \phi_1'(z_2-\mu) - \phi_1'(z_2+\mu) \\ \phi_2'(z_1-\mu) - \phi_2'(z_1+\mu) & \phi_2'(z_2-\mu) - \phi_2'(z_2+\mu) \end{array} \right]$$

where z_1 and z_2 are the locations of the two point actuators (with finite support) and $\phi_i' = \int_{z_j-\mu}^{z_j+\mu} \phi_i(z)dz$. The actuator distribution functions are of the form $b_j(z) = 1/(2\mu)$ for $z \in [z_j - \mu, z_j + \mu]$, where μ is a sufficiently small number, and $b_j(z) = 0$ elsewhere. The explicit form of the nonlinear term $h(a_1, a_2)$ is omitted for brevity.

Following the methodology presented in Section III, we consider an uncertain model of the finite-dimensional system for controller synthesis. The model is of the form of Eq.12 where $\hat{F} = F$, the mismatch between $\widehat{h}(\cdot)$ and $h(\cdot)$ is due to parametric uncertainty in the constant c ($c = 1$ in the model and $c = 0.5$ in the KSE), and $\widehat{G}^k = \left[\begin{array}{ll} \phi_1(z_1^k) & \phi_1(z_2^k) \\ \phi_2(z_1^k) & \phi_2(z_2^k) \end{array} \right]$. Note that the discrepancy between $\widehat{G}^k$ and G^k stems from approximating the actuator distribution functions used in the model by dirac functions. Based on this model, a nonlinear controller that exponentially stabilizes the origin of the closed-loop model is designed using feedback linearization techniques. The controller is designed to place the closed-loop eigenvalues of the model at $(-10, -10)$. Output measurements from two sensors located at $z = -0.25$ and $z = 0.5$ are used to re-set the model state at sampling times. In all simulation runs, the controller is implemented on a 30-th order Galerkin discretization of the KSE. Note that due to the structure of the KSE, the origin is an equilibrium point of both the finite-dimensional slow subsystem and the uncertain model, and therefore we have from Theorem 1 that $L_0^k = 0$, $F_2^k(\Delta) = 0$, and the sampled-data closed-loop system is expected to be asymptotically stable if $F_1^k(\Delta) > 0$.

We consider first the case when no faults are present in the operating actuator configuration, and analyze the dependence of closed-loop stability on the actuator locations and the sampling period. Figs.1(a-c) are contour plots of F_1^k in terms of the locations of the actuators for different sampling periods ($\Delta = 0.25$, 0.75 and 1, respectively). The areas enclosed by the zero contour lines (i.e., the regions where $F_1^k(\Delta) > 0$) represent the set of actuator configurations that enforce asymptotic stability of the closed-loop system. It can be observed from these plots that the set of stabilizing actuator configurations shrinks as the sampling period increases. Fig.1(d) is a contour plot of F_1^k in terms of z_1 and Δ when the location of the second actuator is fixed at $z_2 = 2$. The areas enclosed by the zero contour lines represent the stability regions of the closed-loop system. This plot can be used to determine, for a given sampling period, the range of feasible locations where the first actuator can be placed. Also, for a fixed actuator placement, the boundary point of the zero contour area indicates the maximum stabilizing sampling period.

To illustrate the fault detection and handling capabilities of the sampled-data control system, the system is initialized

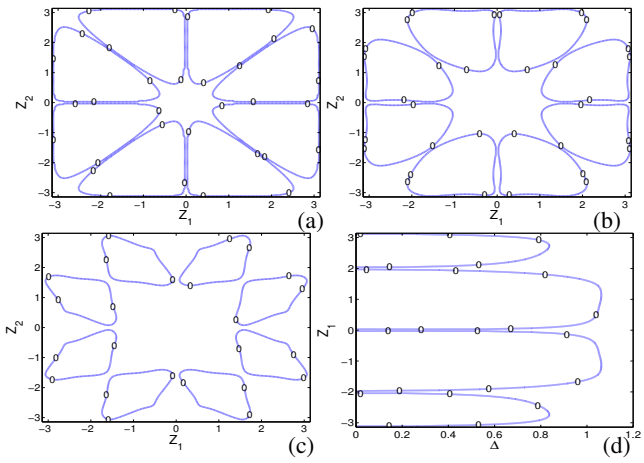

Fig. 1. Plots (a)-(c) depict the sets of stabilizing actuator configurations for $\Delta = 0.25,\ 0.75\ 1$, respectively. Plot (d) shows the range of feasible locations for actuator z_1 on the sampling period for a fixed $z_2 = 2$.

using the healthy actuators placed at $z_1 = -1, z_2 = 2$, and the sampling period is set at $\Delta = 0.25$. To facilitate fault detection, we design a fault-detection filter of the form of Eq.21 based on the model of Eq.11 with L chosen such that the poles of the observer are placed at $(-10, -10)$. Based on the evolution of the residual in the absence of faults, we choose a threshold of $\|r_s(t)\| \leq 0.1$ to detect faults for $t \geq T_b = 0.1$. This allows sufficient time for the fast modes to converge to zero and for the behavior of the infinite-dimensional system to closely follow that of the slow modes. At $T_f = 0.3$, a fault is introduced in the first actuator (see the red line in Fig.2(d)) and the state of the faulty closed-loop system deviates from the zero steady state if no corrective action is taken (see Fig.2(a)). As can be seen from the residual profile in Fig.2(c), the fault is detected at $T_d = 0.75$ when it causes the residual to breach the threshold. The supervisor then needs to switch to a backup actuator to maintain closed-loop stability. For the given sampling period, it can be seen from Fig.1(a) that the actuators placed at $z_1 = 1, z_2 = 1.5$ lie inside the zero contour zone and are therefore expected to be stabilizing. This prediction is confirmed by Fig.2(b) which shows that the backup configuration successfully stabilizes the system at the spatially-uniform steady-state when activated after fault detection (the blue line in Fig.2(d) shows the manipulated input profile of the backup actuator located at $z_1 = 1, z_2 = 1.5$).

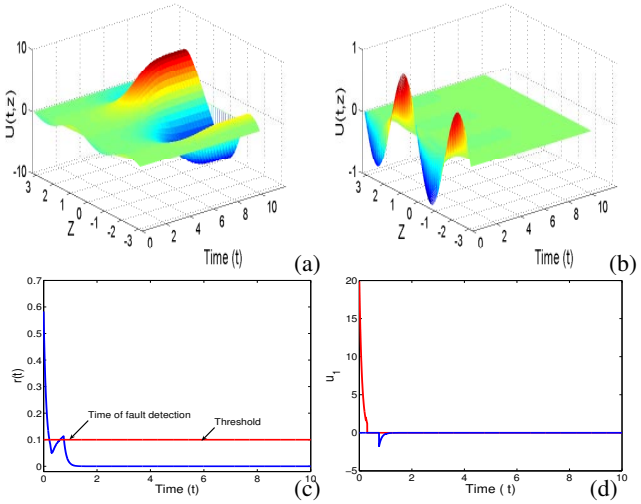

Fig. 2. Plots (a)-(b): Closed-loop state profiles for ($z_1 = -1$, $z_2 = 2$, $\Delta = 0.25$) with failure in first actuator at $T_f = 0.3$ when (a) no corrective action is taken, and (b) switching to a backup configuration ($z_1 = 1$, $z_2 = 1.5$) taks place. Plot (c): Evolution of the residual. Plot (d) Manipulated input profile corresponding for the first actuator in the primary (red) and backup configurations (blue).

REFERENCES

[1] P. M. Frank and X. Ding, "Survey of robust residual generation and evaluation methods in observer-based fault detection systems," *J. Proc. Contr.*, vol. 7, pp. 403–424, 1997.

[2] S. Simani, C. Fantuzzi, and R. Patton, *Model-based Fault Diagnosis in Dynamic Systems Using Identification Techniques*. London: Springer, 2003.

[3] P. Mhaskar, C. McFall, A. Gani, P. D. Christofides, and J. F. Davis, "Isolation and handling of actuator faults in nonlinear systems," *Automatica*, vol. 44, pp. 53–62, 2008.

[4] H. Baruh, "Actuator failure detection in the control of distributed systems," *Journal of Guidance, Control, and Dynamics*, vol. 9, pp. 181–189, 1986.

[5] N. H. El-Farra, Y. Lou, and P. D. Christofides, "Fault-tolerant control of fluid dynamic systems: Coordinated feedback and switching," *Comp. & Chem. Eng.*, vol. 27, pp. 1913–1924, 2003.

[6] A. Armaou and M. Demetriou, "Robust detection and accommodation of incipient component faults in nonlinear distributed processes,," *AIChE J.*, vol. 54, pp. 2651–2662, 2008.

[7] N. H. El-Farra, "Integrated fault detection and fault-tolerant control architectures for distributed processes," *Ind. & Eng. Chem. Res.*, vol. 45, pp. 8338–8351, 2006.

[8] N. H. El-Farra and S. Ghantasala, "Actuator fault isolation and reconfiguration in transport-reaction processes," *AIChE J.*, vol. 53, pp. 1518–1537, 2007.

[9] S. Ghantasala and N. H. El-Farra, "Robust diagnosis and fault-tolerant control of uncertain distributed processes over communication networks," *Int. J. Adapt. Contr. Sig. Proc.*, vol. 23, pp. 699–721, 2009.

[10] ——, "Robust actuator fault isolation and management in constrained uncertain parabolic pde systems," *Automatica*, vol. 45, pp. 2368–2373, 2009.

[11] ——, "Actuator fault detection and reconfiguration in distributed processes with measurement sampling constraints," in *Proceedings of American Control Conference*, St. Louis, MO, 2009, pp. 1523–1529.

[12] L. A. Montestruque and P. J. Antsaklis, "On the model-based control of networked systems," *Automatica*, vol. 39, pp. 1837–1843, 2003.

[13] Y. Sun and N. H. El-Farra, "Quasi-decentralized model-based networked control of process systems," *Comp. & Chem. Eng.*, vol. 32, pp. 2016–2029, 2008.

[14] I. G. Kevrekidis, B. Nicolaenko, and J. C. Scovel, "Back in the saddle again: A computer assisted study of the kuramoto-sivashinsky equation," *SIAM J. Appl. Math.*, vol. 50, pp. 760–790, 1990.

[15] A. Armaou and P. D. Christofides, "Wave suppression by nonlinear finite-dimensional control," *Chem. Eng. Sci.*, vol. 55, pp. 2627–2640, 2000.

[16] W. J. Liu and M. Krstic, "Stability enhancement by boundary control in the kuramoto-sivashinsky equation," *Nonlinear Analysis: Theory, Methods & Applications*, vol. 43, pp. 485–507, 2001.

[17] C. B. Hu and R. Temam, "Robust control of the Kuramoto-Sivashinsky equation," *Dynam. Contin. Dis. & Impul. Syst. (Series B)*, vol. 8, pp. 315–338, 2001.

[18] Y. Sun and N. H. El-Farra, "Resource-aware quasi-decentralized control of nonlinear plants over communication networks," in *Proceedings of American Control Conference*, St. Louis, MO, 2009, pp. 154–159.

[19] H. K. Khalil, *Nonlinear Systems*, 2nd ed. Upper Saddle River, New Jersey: Prentice Hall, 1996.

[20] P. D. Christofides, *Nonlinear and Robust Control of PDE Systems: Methods and Applications to Transport-Reaction Processes*. Boston: Birkhäuser, 2001.